Robustness of flow networks against cascading failures under partial load redistribution

Omur Ozel, Bruno Sinopoli, Osman Yağan
Department of ECE, Carnegie Mellon University, Pittsburgh, PA 15213 USA

(Dated: February 23, 2018)

We study the robustness of flow networks against cascading failures under a *partial* load redistribution model. In particular, we consider a flow network of N lines with initial loads $L_1, \ldots, L_N$ and free-spaces $S_1, \ldots, S_N$ that are independent and identically distributed with joint distribution $P_{LS}(x,y) = \mathbb{P}[L \leq x, S \leq y]$. The *capacity* C_i is the maximum load allowed on line i, and is given by $C_i = L_i + S_i$. When a line fails due to overloading, it is removed from the system and $(1-\varepsilon)$-fraction of the load it was carrying (at the moment of failing) gets redistributed *equally* among all remaining lines in the system; hence we refer to this as the *partial* load redistribution model. The rest (i.e., ε-fraction) of the load is assumed to be *lost* or *absorbed*, e.g., due to advanced circuitry disconnecting overloaded power lines or an *inter-connected* network/material absorbing a fraction of the flow from overloaded lines. We analyze the robustness of this flow network against *random* attacks that remove a *p-fraction* of the lines. Our contributions include (i) deriving the *final* fraction of alive lines $n_\infty(p,\varepsilon)$ for all $p, \varepsilon \in (0,1)$ and confirming the results via extensive simulations; (ii) showing that partial redistribution might lead to (depending on the parameter $0 < \varepsilon \leq 1$) the order of transition at the critical attack size $p^\star$ changing from first to second-order; and (iii) proving analytically that the widely used robustness metric measuring the area $\int_0^1 n_\infty(p,\varepsilon)\mathrm{d}p$ is maximized when all lines have the same free-space regardless of their initial load.

PACS numbers: 64.60.Ht, 62.20.M-, 89.75.-k, 02.50.-r

I. INTRODUCTION

Flow network abstractions have been extensively used to analyze complex system phenomena occurring in power line networks, financial networks, transportation networks and biological ecosystems. Current trends in the technological development such as online social media, cyber-physical systems and the internet of things have enabled a plethora of new applications involving dynamical interactions over and within flow networks. In this respect, current research on networks cover phenomena such as information dissemination and influence propagation [1–5], percolation [6–11] and robustness [12–18]. In this paper, our focus is on robustness of flow networks.

A flow network is typically susceptible to cascading failures. An event of at least one failure of a line in a flow network could trigger failure of the others and a significant portion of lines in the network could fail in what has been identified in the literature as the cascading failures. Real life phenomena such as blackouts in power networks [19] and financial crisis in financial networks [20] occur as a consequence of rapid failures that follow one after the other. Consequently, understanding possible mechanisms of such failures is of paramount importance, see e.g. [21]. Robustness of flow network structures against cascading failures is an active research topic and has received recent interest from many researchers [12–14]. For example, [22–24] consider power networks where the failure mechanism is the equal redistribution of load upon the failure of a power line. We consider a similar phenomenon in flow networks. In particular, we build our analysis upon the well known fiber-bundle model [25]. Fiber bundle models have been used in a wide range of applications including fatigue [26], failure of composite materials [27] and landslides [28].

Flow networks typically include built-in systems to counter cascade formations and alleviate the spread of the adverse effect of failures over other lines in the network [18]. In this paper, our objective is to obtain a unified understanding of cascading failures for networks with a specific mechanism to counter such failures. In particular, we study the robustness under *partial* load redistribution in a *democratic fiber bundle-like* model. Our problem setting is as follows: We consider N lines whose initial loads $L_1, \ldots, L_N$ and free-spaces $S_1, \ldots, S_N$ have joint distribution $P_{LS}(x,y) = \mathbb{P}[L \leq x, S \leq y]$ and independent and identically distributed along lines. The maximum flow allowed on a line i defines its *capacity*, and is given by $C_i = L_i + S_i$. When a line fails due to overloading, it is removed from the system and $(1-\varepsilon)$-fraction of the load it was carrying (at the moment of failing) gets redistributed *equally* among all remaining lines in the system; hence we refer to this as the *partial* load redistribution model. The rest (i.e., ε-fraction) of the load is assumed to be *lost* or *absorbed*, e.g., due to advanced circuitry disconnecting overloaded power lines or an *inter-connected* network/material absorbing a fraction of the flow from overloaded lines.

We study the robustness of the flow network described above against *random* malicious attacks (or, failures) that remove a *p-fraction* of the lines from the system. Note that the *full-redistribution* case $\varepsilon = 0$ was studied in [29] where it was shown that the transition of $n_\infty(p)$ at the critical point $p^\star$ is always first order; and $n_\infty(p)$ is maximized for all attack sizes $0 < p < 1$ when free-space S follows a Dirac-delta distribution. In the current paper, we derive the *final* fraction of alive lines $n_\infty(p,\varepsilon)$ for all $p,\varepsilon \in (0,1)$. We obtain an iterative relation that characterizes the dynamical extra load that is added per line and we confirm the results via extensive simulations. In our numerical results, we observe that the order of transition at $p^\star$ changes from first to second-order after ε exceeds a certain *tricritical* point. Additionally, we observe that for arbitrary $\varepsilon > 0$, the Dirac delta distribution on S does not necessarily maximize $p^\star$ as was the case when $\varepsilon = 0$ (under fixed $\mathbb{E}[L]$ and $\mathbb{E}[S]$).

Next, we investigate the robustness of the flow network and its variation with respect to ε. Different from the earlier work in [29], in the current paper, we consider a metric that measures the area $\int_0^1 n_\infty(p,\varepsilon)\mathrm{d}p$ which was originally proposed in [30]. We provide a complete mathematical proof that this robustness metric is maximized when all lines have the same free-space regardless of their initial load. That is, this metric is maximized when the free-space distribution is a Dirac delta function centered at $\mathbb{E}[S]$, irrespective of the parameter ε and how initial loads L_i are distributed. This result holds true despite the fact that the critical attack size $p^\star$ is not necessarily maximized under the same Dirac delta distribution. This result extends previous findings due to [29] for the robustness metric $\int_0^1 n_\infty(p,\varepsilon)\mathrm{d}p$ when a portion of the load is absorbed or lost in the redistribution process. We believe that our results provide interesting insights into the dynamics of cascading failures in flow networks with partial load absorption or loss mechanism in redistribution.

The rest of the paper has the following format. In Section II, we explain the system model in details, discuss how it extends other models in the literature, and present the problem definition. In Section III, we obtain an iterative dynamical relation for the extra load per alive line at every stage of the cascading failure process, under general load and free-space distributions. Section IV is devoted to numerical results that confirm the main findings of the paper for systems of finite size. In Section V, we provide a complete mathematical treatment to derive the optimal distribution of load and free-space (when mean values of both are fixed) that leads to maximum robustness. In Section VI, we conclude our paper.

II. MODEL AND PROBLEM DEFINITION

Partial load-redistribution model. We consider a network with N lines $\mathcal{L}_1,\ldots,\mathcal{L}_N$ with initial loads $L_1,\ldots,L_N$. The *capacity* C_i of a line $\mathcal{L}_i$ defines the maximum power flow that can be carried by it, and is expressed as

$$C_i = L_i + S_i, \qquad i = 1,\ldots,N, \tag{1}$$

where S_i denotes the *free-space* that is assigned to line $\mathcal{L}_i$. Alternatively, the capacity of a line $\mathcal{L}_i$ can be defined as a factor of its initial load, i.e.,

$$C_i = (1+\alpha_i)L_i \tag{2}$$

with $\alpha_i > 0$ denoting its *tolerance* factor. Accordingly, the extra load space S_i is given in terms of the initial load L_i as $S_i = \alpha_i L_i$. Most existing works assume a *fixed* tolerance factor for all lines in the system, i.e., $\alpha_i = \alpha$ for all i; e.g., see [31–34].

The main assumption of our model is that when a line fails due to *overloading*, i.e., due to its load exceeding its capacity, it is removed from the system and $(1-\varepsilon)$-fraction of the load it was carrying (at the moment of failing) gets redistributed *equally* among all remaining lines in the system; hence we refer to this as the *partial* load redistribution model. The rest (i.e., ε-fraction) of its load is assumed to be *lost* or *absorbed*.

The partial load redistribution model is motivated by several real-world scenarios. For instance, most real-world power systems are equipped with advanced protection circuits that immediately disconnect the overloaded lines from the rest of the grid [35, 36]; the parameter ε would then represent the fraction of lines protected by such advanced circuitry. Alternatively, we can think of a flow network (resp. a bundle of fibers) that is *inter-connected* with another network (resp. material) that can absorb a fraction of the flow from overloaded lines.

Throughout we assume that the pairs (L_i, S_i) are independently and identically distributed (i.i.d.) with the joint distribution $P_{LS}(x,y) := \mathbb{P}[L \le x, S \le y]$ for each $i = 1,\ldots,N$. The corresponding joint probability density function is given by $p_{LS}(x,y) = \frac{\partial^2}{\partial x \partial y}P_{LS}(x,y)$. We assume that the marginal densities $p_L(x)$ and $p_S(y)$ are continuous on their support. L_{min} and S_{min} denote the minimum values for load L and extra load space S, respectively, throughout the paper; i.e.,

$$L_{min} = \inf\{x : P_L(x) > 0\}$$
$$S_{min} = \inf\{y : P_S(y) > 0\}$$

We assume that $L_{min}, S_{min} > 0$.

Our load redistribution model is intimately related to the *democratic* fiber bundle model [23, 24] where N parallel fibers with failure thresholds $C_1,\ldots,C_N$ share an applied total force F *equally*. In this line of literature, it has been of interest to study the dynamics of recursive failures in the bundle as the applied force F increases; e.g., see [37–39]. This model was used by [22] in the context of power line networks, with F corresponding to the total load shared *equally* by N power lines. See also [29] for the latest developments on the democratic fiber bundle model relating to a power line network. The relevance of the equal load-redistribution model for power systems stems from its relation to the Kirchhoff's law in the mean-field sense. Our current partial load redistribution model builds upon that in [29]. Even though our model involves a *global* redistribution of a fraction of the extra load due to line failures, the capability to partially capture the failures is, in effect, due to the ability to keep a portion of the extra load due to failed lines in a *local* level, possibly in a secondary network. While our current work does not consider the interaction of local and global behavior, our framework helps build a step towards this direction.

Problem definition. Our main goal is to study the robustness of the flow network under the partial load redistribution rule described above. We consider a *random* attack or a random failure that leads to p-fraction of the lines to be removed from the system. We assume that the load of these initially failed lines are redistributed *in full* to the non-attacked lines, with each non-attacked line receiving an equal portion of the total load failed. Our motivation in distinguishing these initial failures (resulting from an attack) from failures due to overloading of lines is two-fold. Firstly, in the case of a physical attack to the system, we would expect any advanced circuitry or inter-connection to other networks to be damaged along with the failed lines, making it impossible for ε-fraction of the failed load to be absorbed. Secondly, this assumption ensures that a random attack against p-fraction of the lines is equivalent (in the mean-field sense) to a disturbance caused by increasing the initial load of every line (or, force applied to every fiber) by $p\mathbb{E}[L]/(1-p)$. This in turn enables our analysis to provide insights on the robustness of the system against both random attacks (as commonly considered in the context of power systems) as well as the increase of total applied load or force (as commonly considered in the context of fiber bundles).

After the initial load redistribution, the amount of load on each alive line will be given by its initial load plus its share of the total load of the failed lines. This, in turn, leads to the failure of additional lines due to the updated flow exceeding their capacity. In the ensuing stages of this process, the network is assumed to have the capability of *absorbing* (i.e., removing from the system) ε-fraction of the load from lines who fail due to overloading. Put differently, if a line $\mathcal{L}_i$ fails due to its load $L_i(t)$ at time t exceeding its capacity, then only $(1-\varepsilon)L_i(t)$ amount of load will be redistributed, in an equal manner, to the remaining lines; as mentioned before, the system is assumed to absorb the portion $\varepsilon L_i(t)$ either by help of advanced circuitry or by means of shedding that portion of load to an inter-connected system.

In the most general scenario for partial redistribution, we could allow ε to depend on time t and the extra load incurred per line at that time. However, our main goal for analysis in this paper is to understand the case when ε is constant throughout time. The load redistribution process continues recursively until no further failures occur, potentially generating a *cascade of failures*. Our goal is to understand the limits associated with this process. We let $n_\infty(p,\varepsilon)$ denote the *final* (i.e., steady-state) fraction of alive lines when a p-fraction of lines is randomly attacked initially; as before ε denotes the fraction of flow from *overloaded* lines that will be lost (and thus will not be redistributed to the remaining lines) at each stage of the cascade process.

The main goal of the paper is to derive expressions for $n_\infty(p,\varepsilon)$ for all attack sizes $0<p<1$ and any $0\le\varepsilon\le 1$ in order to understand the *robustness* of the network under the partial load redistribution model. We will be particularly interested in understanding the *critical* attack size $p^\star$ at which $n_\infty(p,\varepsilon)$ drops to zero, and in developing design guidelines (e.g., in the sense of choosing the distribution p_{LS}) to optimize network robustness under given constraints.

Related work. The problem formulation considered here was introduced by Yağan [3] and then later extended in [29]. As such, our current work could be viewed as an extension of these works in the literature. Our current formulation differs from the democratic fiber bundle-like model in [29] in that there is a load recapture capability ε in the system and this difference deems the load dynamics and resulting analysis of the problem significantly harder than that in the previous work [3, 29].

With regard to the notation in use: The random variables (rvs) under consideration are all defined on the same probability space $(\Omega,\mathcal{F},\mathbb{P})$. Probabilistic statements are made with respect to this probability measure $\mathbb{P}$, and we denote the corresponding expectation operator by $\mathbb{E}$. The indicator function of an event A is denoted by $\mathbf{1}[A]$.

III. ANALYTIC RESULTS

In this section, we provide a mean-field analysis for the cascading failures of lines under the model described in Section II. We start by deriving recursive relations concerning the fraction f_t of lines that are *failed* at time stage $t=0,1,\ldots$. The number of links that are still alive at time t is then given by $N_t=N(1-f_t)$ for all $t=0,1,\ldots$. The cascading failures start with a random attack that targets a fraction p of lines. Hence, we have $f_0=p$. Upon the failure of these f_0 lines, their load will be redistributed to the remaining $(1-f_0)N$ lines, with each remaining line receiving an equal portion of the failed load. Since the pN lines that have been attacked are selected uniformly at random, the mean total load that will be redistributed to the remaining lines is given by $\mathbb{E}[L]\,pN$. The resulting extra load per alive line, Q_0, is thus given by

$$Q_0=\frac{\mathbb{E}[L]\,pN}{(1-p)N}=\mathbb{E}[L]\,\frac{f_0}{1-f_0}. \tag{3}$$

In the next stage, a line i that survives the initial attack fails when its new load reaches its capacity. For convenience, we assume that a line also fails when its load equals its capacity, i.e., when

$$L_i+Q_0\ge L_i+S_i,$$

or, equivalently $S_i\le Q_0$. Therefore, at stage $t=1$, an additional fraction $\mathbb{P}[S\le Q_0]$ of the lines that were alive at the end of stage 0 fail. This yields

$$f_1=f_0+(1-f_0)\mathbb{P}[S\le Q_0]=1-(1-f_0)\mathbb{P}[S>Q_0]\,.$$

Now, to compute the extra load per alive line at stage 1, which we denote by Q_1, we need to sum the total load of the lines failed precisely at stage 1, multiply it by $(1-\varepsilon)$ to account for the load absorbed or lost as explained in Section II, divide it by the new system size $(1-f_1)N$ and add this fraction on top of the existing extra load. With $\mathcal{A}$ denoting the initial set of lines attacked, this gives

$$\begin{aligned} Q_1 &= Q_0 + \frac{1-\varepsilon}{(1-f_1)N} \cdot \mathbb{E}\left[\sum_{i\notin\mathcal{A}:S_i\le Q_0} (L_i+Q_0)\right] \\ &= Q_0 + \frac{1-\varepsilon}{(1-f_1)N} \cdot \sum_{i\notin\mathcal{A}} \mathbb{E}\left[(L_i+Q_0)\mathbf{1}\left[S_i \le Q_0\right]\right] \\ &= Q_0 + (1-\varepsilon)(1-f_0)\frac{\mathbb{E}\left[(L+Q_0)\cdot\mathbf{1}\left[S\le Q_0\right]\right]}{1-f_1}, \end{aligned}$$

where the last step uses $|\mathcal{A}|/N = p = f_0$.

At the stage $t=2$, the following two conditions are needed for a line to still stay alive: i) it should not have failed until this stage, which happens with probability $1-f_1$ and necessitates its free-space to satisfy $S > Q_0$; and ii) its free-space should also satisfy $S > Q_1$ so that its capacity is still larger than its current load. Thus, the fraction of failures f_2 at this stage is given by

$$f_2 = 1-(1-f_1)\mathbb{P}\left[S > Q_1 \mid S > Q_0\right].$$

On the other hand, we can calculate the total load that is redistributed to the remaining lines as before:

$$Q_2 = Q_1 + (1-\varepsilon)(1-f_0)\frac{\mathbb{E}\left[(L+Q_1)\cdot\mathbf{1}\left[Q_0 < S \le Q_1\right]\right]}{1-f_2}.$$

The form of the recursive equations for each $t=0,1,\dots$ can now be seen to be as follows:

$$\begin{aligned} f_{t+1} &= 1-(1-f_t)\mathbb{P}\left[S > Q_t \,\middle|\, S > Q_{t-1}\right] \\ Q_{t+1} &= Q_t + (1-\varepsilon)(1-f_0)\tfrac{\mathbb{E}\left[(L+Q_t)\cdot\mathbf{1}\left[Q_{t-1}<S\le Q_t\right]\right]}{1-f_{t+1}} \\ N_{t+1} &= (1-f_{t+1})N \end{aligned} \tag{4}$$

where $f_0 = p$, $N_0 = N(1-p)$, and $Q_0 = \mathbb{E}\left[L\right]\frac{p}{1-p}$. For convenience, we also let $Q_{-1}=0$. From (4) we see that cascades stop and a steady state is reached, i.e., $N_{t+2} = N_{t+1}$, if

$$\mathbb{P}\left[S > Q_{t+1} \,\middle|\, S > Q_t\right] = 1. \tag{5}$$

We now work towards simplifying the recursion on Q_t in order to obtain a better understanding of the condition (5) needed for cascading failures to stop. To this end, we apply the first relation in (4) repeatedly to see that

$$\begin{aligned} 1-f_{t+1} &= (1-f_t)\mathbb{P}\left[S > Q_t \mid S > Q_{t-1}\right] \\ 1-f_t &= (1-f_{t-1})\mathbb{P}\left[S > Q_{t-1} \mid S > Q_{t-2}\right] \\ &\ \ \vdots \\ 1-f_2 &= (1-f_1)\mathbb{P}\left[S > Q_1 \mid S > Q_0\right] \\ 1-f_1 &= (1-f_0)\mathbb{P}\left[S > Q_0\right]. \end{aligned}$$

Applying these recursively starting from the last equality, we find that

$$1-f_{t+1} = (1-f_0)\prod_{\ell=0}^{t}\mathbb{P}\left[S > Q_\ell \mid S > Q_{\ell-1}\right],$$

where we set $Q_{-1}=0$ as before. Since Q_t is monotone increasing in t, i.e., $Q_{t+1}\ge Q_t$ for all t, we further obtain

$$\begin{aligned} &1-f_{t+1} \\ &= (1-f_1)\frac{\mathbb{P}\left[S>Q_t\right]}{\mathbb{P}\left[S>Q_{t-1}\right]}\cdot\frac{\mathbb{P}\left[S>Q_{t-1}\right]}{\mathbb{P}\left[S>Q_{t-2}\right]}\cdots\frac{\mathbb{P}\left[S>Q_1\right]}{\mathbb{P}\left[S>Q_0\right]} \\ &= (1-p)\mathbb{P}\left[S>Q_t\right] \end{aligned} \tag{6}$$

This last expression confirms the intuitive result that the fraction of alive lines at stage $t+1$ is simply given by the fraction of lines who survive the initial attack and have more free-space than the extra load Q_t that is distributed on every alive line at stage t.

Using (6) in (4), it is now understood that the dynamics of cascading failures is fully governed and understood by the recursions on Q_t given by

$$Q_{t+1} = Q_t + (1-\varepsilon)\frac{\mathbb{E}\left[(L+Q_t)\cdot\mathbf{1}\left[Q_{t-1}<S\le Q_t\right]\right]}{\mathbb{P}\left[S>Q_t\right]} \tag{7}$$

for each $t=0,1,\dots$ (with Q_0 given at (3)), with the condition for reaching the steady-state still being (5). Let $t^\star$ be the stage at which steady-state is reached, i.e., the first t for which (5) holds. Then, the final system sizes $n_\infty(p,\varepsilon)$ defined as the fraction of alive lines at the steady state can be computed simply from (viz. (6))

$$n_\infty(p,\varepsilon) = (1-p)\mathbb{P}\left[S > Q_{t^\star}\right]. \tag{8}$$

Throughout, we will be particularly interested in the critical attack size $p^\star$ defined as the largest attack that the system can sustain (in the sense of having a positive final size $n_\infty(p,\varepsilon)$); i.e., for given ε we let

$$p^\star(\varepsilon) = \sup\{p>0 : n_\infty(p,\varepsilon) > 0\}$$

In order to demonstrate the impact of the loss factor ε together with the number of stages needed to reach a steady-state, we find it useful to further simplify (7). By simple algebra, we get

$$\begin{aligned} &Q_{t+1}\mathbb{P}\left[S>Q_t\right] \\ &= Q_t\mathbb{P}\left[S>Q_t\right] + (1-\varepsilon)Q_t\mathbb{P}\left[Q_{t-1}<S\le Q_t\right] \\ &\quad + (1-\varepsilon)\mathbb{E}\left[L\cdot\mathbf{1}\left[Q_{t-1}<S\le Q_t\right]\right] \\ &= Q_t\mathbb{P}\left[S>Q_{t-1}\right] - \varepsilon Q_t\mathbb{P}\left[Q_{t-1}<S\le Q_t\right] \\ &\quad + (1-\varepsilon)\mathbb{E}\left[L\cdot\mathbf{1}\left[Q_{t-1}<S\le Q_t\right]\right], \end{aligned}$$

which is equivalent to the following difference relation on the sequence $Q_{t+1}\mathbb{P}\left[S>Q_t\right]$

$$\begin{aligned} &Q_{t+1}\mathbb{P}\left[S>Q_t\right] - Q_t\mathbb{P}\left[S>Q_{t-1}\right] \\ &= (1-\varepsilon)\mathbb{E}\left[L\mathbf{1}\left[Q_{t-1}<S\le Q_t\right]\right] - \varepsilon Q_t\mathbb{P}\left[Q_{t-1}<S\le Q_t\right] \end{aligned} \tag{9}$$

We see from (9) that higher values of ε have suppressing effect on the growth of Q_t, leading to steady-state being reached *faster* (i.e., in small number of steps), and with a larger final system size in view of (8).

It is desirable to obtain a closed-form solution for $Q_{t^\star}$ by solving the difference equation (8); in view of (8) this would lead to a closed-form expression for the final system size $n_\infty(p,\varepsilon)$. However, applying (9) recursively leads to a telescoping sum given by

$$Q_{t+1}\mathbb{P}\left[S > Q_t\right] - Q_0 = (1-\varepsilon)\sum_{i=0}^{t}\mathbb{E}\left[L \cdot \mathbf{1}\left[Q_{i-1} < S \le Q_i\right]\right] - \varepsilon \sum_{i=0}^{t} Q_i \mathbb{P}\left[Q_{i-1} < S \le Q_i\right] \quad (10)$$

It is now clear that unless $\varepsilon = 0$ or $\varepsilon = 1$, a direct expression for Q_t (for arbitrary t) can not be obtained without going through the recursion (9) and obtaining each one of $Q_1, Q_2, \ldots, Q_{t-1}$. Therefore, it is also not possible to derive a closed-form expression for $Q_{t^\star}$ and $n_\infty(p,\varepsilon)$.

IV. NUMERICAL RESULTS

In this section, we confirm our theoretical findings via numerical simulations. We focus on three commonly known distributions for the load and free-space variables: i) Uniform, ii) Pareto, and iii) Weibull. The probability density functions corresponding to these distributions are given below for a generic random variable L.

- Pareto Distribution: $L \sim \mathit{Pareto}(L_{\min}, b)$. With $L_{\min} > 0$ and $b > 0$, the support set is $x \ge L_{min}$ and the density is given by

$$p_L(x) = L_{\min}^b b x^{-b-1}.$$

  We also enforce $b > 1$ in order to ensure that $\mathbb{E}\left[L\right] = bL_{\min}/(b-1)$ is finite. The Pareto family distributions are also known as *power-law* distributions and have been extensively used in many fields.

- Uniform Distribution: $L \sim U(L_{\min}, L_{\max})$. The support set is $L_{min} \le x \le L_{max}$ and the density is given by

$$p_L(x) = \frac{1}{L_{\max} - L_{\min}}$$

- Weibull Distribution: $L \sim \mathit{Weibull}(L_{\min}, \lambda, k)$. With $\lambda, k, L_{\min} > 0$, the support set is $x \ge L_{min}$ and the density is given by

$$p_L(x) = \frac{k}{\lambda}\left(\frac{x - L_{\min}}{\lambda}\right)^{k-1} e^{-\left(\frac{x-L_{\min}}{\lambda}\right)^k}.$$

  The case $k = 1$ corresponds to the exponential distribution, and $k = 2$ corresponds to Rayleigh distribution. The mean load is given by $\mathbb{E}\left[L\right] = L_{\min} + \lambda\Gamma(1 + 1/k)$, where $\Gamma(\cdot)$ is the gamma-function $\Gamma(x) = \int_0^\infty t^{x-1}e^{-t}dt$.

Next, we confirm our results presented in Section III concerning the response of the system to attacks of varying sizes; i.e., concerning the final system size $n_\infty(p,\varepsilon)$. We are particularly interested in the transition behavior around the critical attack size $p^\star$. In all simulations,

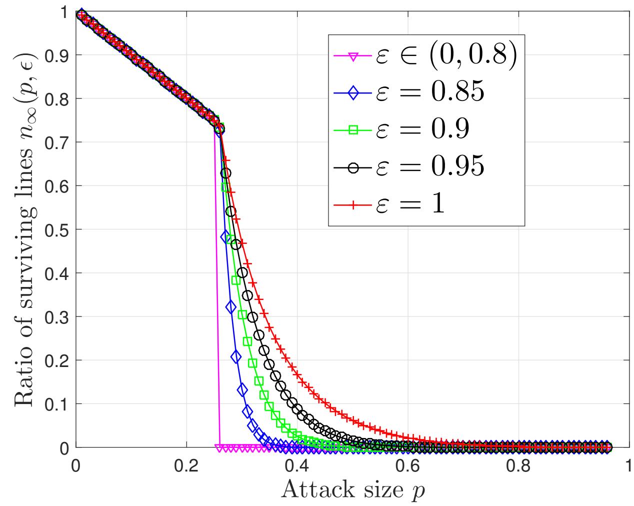

FIG. 1. *The breakdown of the system is demonstrated, where $L_1, \ldots, L_N$ are drawn from Pareto distribution with $b = 2$, $L_{min} = 10$. We also have $S = 0.7L$ so that $S_1, \ldots, S_N$ are such that $S_i = 0.7L_i$. We plot the ratio of surviving lines $n_\infty(p,\varepsilon)$ as a function of the attack size p for various ε values.*

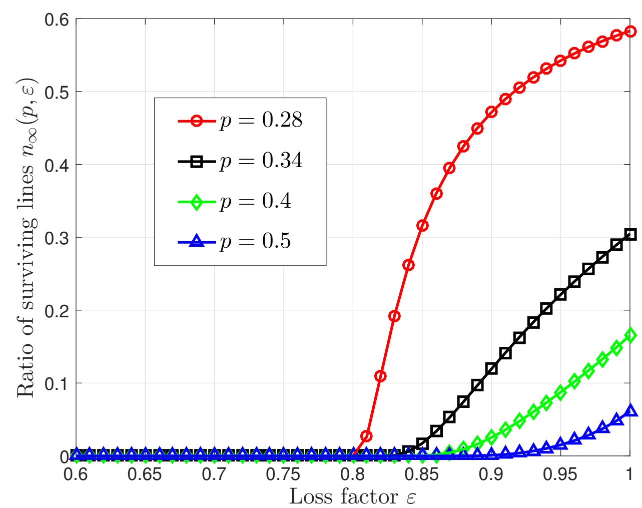

FIG. 2. *In the setting of Fig. 1, we plot the relative final size $n_\infty(p,\varepsilon)$ as a function of the loss factor parameter ε for different attack sizes p.*

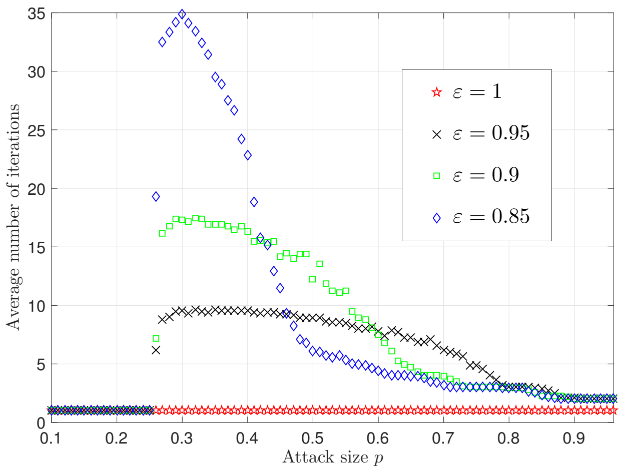

FIG. 3. *In the setting of Fig. 1, we plot the average number of iterations needed for convergence as a function of the attack size p for various ε values.*

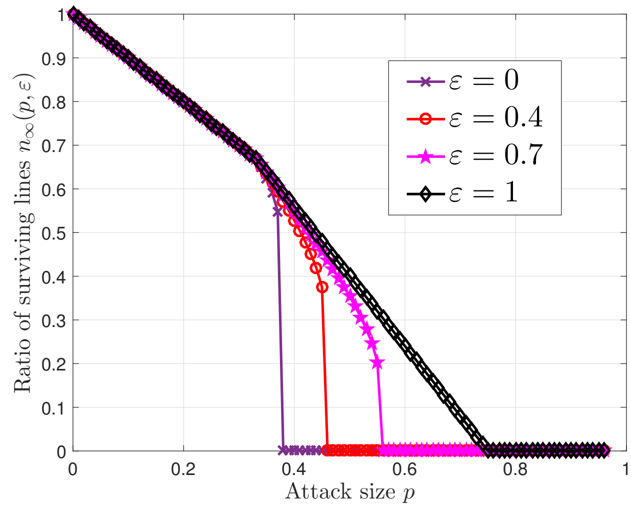

FIG. 4. *The breakdown of the system is demonstrated, where $L_1, \ldots, L_N$ are drawn independently from a uniform distribution with $L_{min} = 10$ and $\mathbb{E}[L] = 20$, and $S_1, \ldots, S_N$ are drawn independently from a uniform distribution with $S_{min} = 10$ and $\mathbb{E}[S] = 35$. We plot the relative final size $n_\infty(p,\varepsilon)$ as a function of the attack size p for different ε.*

we fix the number of lines at $N = 10^6$, and for each set of parameters being considered (e.g., the distribution $p_{LS}(x, y)$ and attack size p) we run 200 independent experiments. In all figures below, the symbols represent the *empirical* value of the final system size $n_\infty(p,\varepsilon)$ (obtained from simulations by averaging over 200 independent runs for each data point), and solid lines represent the analytic results computed from (8) with $Q_{t^\star}$ obtained by iterating (7) while checking the condition (5) at each iteration step.

We start our numerical results with Pareto distribution. In Figs. 1 - 3, we let $L_1, \ldots, L_N$ be drawn from Pareto distribution with $b = 2$, $L_{\min} = 10$ and $S = 0.7L$. In Fig. 1, we plot the ratio of surviving lines $n_\infty(p,\varepsilon)$ as a function of the attack size p for various ε values. We already know from the analysis in [3] that for $\varepsilon = 0$, Pareto distribution always fosters an abrupt first-order transition behavior at $p^\star$. We observe that this first order transition behavior continues to hold as ε is increased from 0 to 0.8. In fact, up until that point, the system's ability to absorb ε-fraction of the failed load at each stage does not affect the final system size $n_\infty(p,\varepsilon)$. Only after $\varepsilon = 0.8$ the behavior of $n_\infty(p,\varepsilon)$ starts to change as shown in Fig. 1. For a complementary visualization, we plot the behavior of the ratio of surviving node $n_\infty(p,\varepsilon)$ as a function of ε for different values of initial attack size p. We see that the transition no longer fosters any sharp behavior and continuously improves as it reaches $\varepsilon = 1$. We next provide the mathematical justification for this observation.

When $\varepsilon = 1$, an overloaded line will be removed from the system *without* its load being redistributed to the remaining lines. Put differently, the only time redistribution will take place is stage 1, where Q_0 gets redistributed to each of the $(1-p)N$ lines that have not been attacked. Therefore, a line that is not in the initial attack will be included in the final system size as long as its free-space is larger than Q_0. This leads to having

$$n_\infty(p,\varepsilon) = (1-p)\mathbb{P}[S > Q_0] \tag{11}$$

where $Q_0 = \frac{p}{1-p}\mathbb{E}[L]$. Therefore, $n_\infty(p,\varepsilon)$ is continuous in p whenever the marginal distribution of S is continuous, a condition satisfied in all distributions considered in the numerical results. Therefore, in the case of perfect ε, $n(p,\varepsilon)$ hits zero and the system fully collapses in a continuous fashion. We further note that the distribution of S under fixed $\mathbb{E}[L]$ and $\mathbb{E}[S]$ can be selected so that the critical attack size $p^\star$ can be made arbitrarily close to 1. Selecting S as a binary random variable at $\{s_1, s_2\}$ with $s_1 < \mathbb{E}[S] < s_2$ independent from L such that $p_1 s_1 + p_2 s_2 = \mathbb{E}[S]$ is sufficient to see this phenomenon. For fixed $s_1 < \mathbb{E}[S]$, one can select s_2 arbitrarily large with $p_1, p_2 \neq 0$ such that $p_1 s_1 + p_2 s_2 = \mathbb{E}[S]$ and this proves that $\mathbb{P}[S > Q_0]$ can be made non-zero *irrespective of the value of the initial attack size* p, i.e., $p^\star$ can be made arbitrarily close to 1.

In Fig. 3, we observe that the number of iterations for convergence is affected significantly by introducing the parameter ε. In particular, the number of iterations foster a smoother variation as ε is increased. Finally, the number of iterations converge uniformly to 1 as ε tends to 1 as further iterations simply stop in this perfect scenario.

In Fig. 4, we plot the ratio of surviving lines $n_\infty(p,\varepsilon)$ with respect to p when $L_1, \ldots, L_N$ are drawn from the load L and extra space S is independent and uniformly distributed with $L_{min} = S_{min} = 10$ and $\mathbb{E}[L] = 20$ and $\mathbb{E}[S] = 35$. We observe that the transition behavior has a failure with preceding divergence and the critical threshold $p^\star$ migrates from $p^\star(\varepsilon) = 0.375$ at $\varepsilon = 0$ to

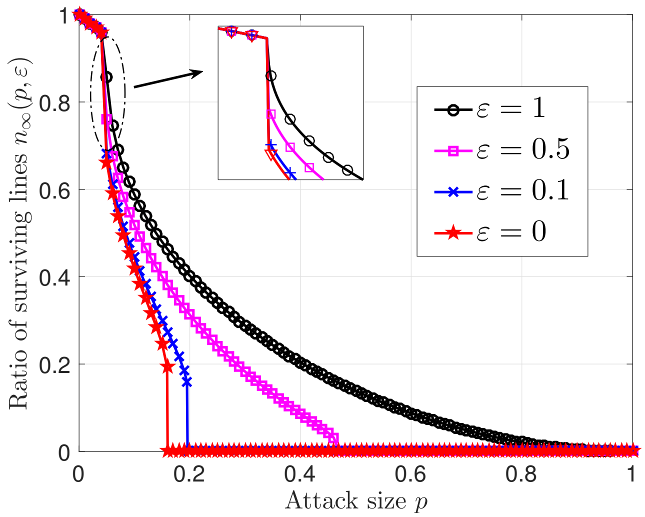

FIG. 5. *The breakdown of the system is demonstrated, where $L_1, \ldots, L_N$ are drawn from Weibull distribution with $k = 0.4$, $\lambda = 100$, $L_{min} = 10$, and free-space for each lines is given by $S = 1.74L$. We plot the ratio of surviving lines $n_\infty(p,\varepsilon)$ as a function of the attack size p.*

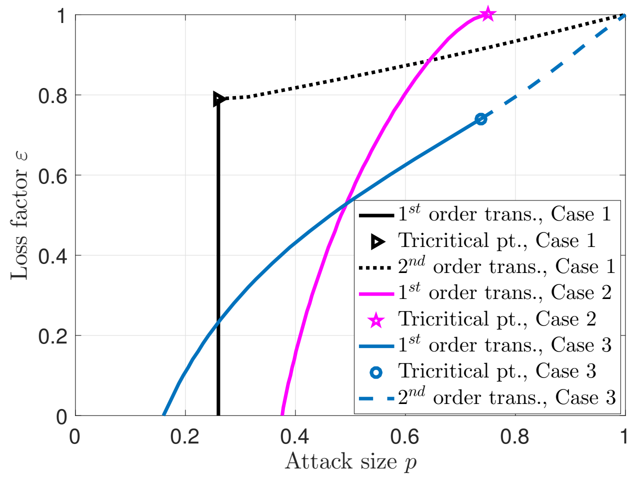

FIG. 6. *The phase diagrams and the resulting tricritical behavior is shown for Cases 1, 2 and 3 that correspond the settings in Figs. 1, 4, and 5, respectively. For each value of the loss factor ε, we show the corresponding* critical *attack size p. Solid curves represent cases where the transition at the corresponding critical attack size is first-order, while dashed curves stand for cases where a second-order phase transition occurs.*

$p^\star(\varepsilon) = 0.75$.

In Fig. 5, we plot the ratio of surviving lines $n_\infty(p,\varepsilon)$ with respect to p when $L_1, \ldots, L_N$ are drawn from Weibull distribution with $k = 0.4$, $\lambda = 100$, $L_{\min} = 10$, $S = 1.74L$. We see that the Weibull distribution gives rise to a richer set of possibilities for the transition of $n_\infty(p,\varepsilon)$. Namely, we see that an abrupt rupture, a rupture with preceding divergence as well as a first-order transition followed by a second-order transition that is followed by an ultimate first-order breakdown are all possible in this case. As the parameter ε is increased, the transition behavior gets smoother.

We finally examine the phase diagrams corresponding to cases presented above and reveal the emergence of tricritical points. In Fig. 6, we plot the loss factor ε and attack size p pairs for which the phase transition occurs in either first or second order. We denote a first order transition by straight line and a second order transition by dashed line. In Fig. 6, we refer to the case of $L \sim$ Pareto(2,10) and $S = 0.7L$ as Case 1, the case of independent L, S with $L \sim$ Uniform([10,30]) and $S \sim$ Uniform([10,60]) as Case 2 and the case of $L \sim$ Weibull(10,100,0.4) and $S = 1.74L$ as Case 3. We observe that Case 1 fosters a very sharp phase diagram in that the phase transition occurs at the same attack size for all loss factors smaller than a certain ε and disappears after that. In contrast, Case 2 has a smoother phase diagram as the phase transition switches from first order to second order after a certain tricritical point [40]. We also observe that the transition in Case 3 is always of first order and the corresponding phase diagram is smooth.

V. OPTIMIZING ROBUSTNESS

A typical metric to assess network robustness is the percolation threshold $p^\star$ at which the system fully collapses as a result of the cascading failures [3, 29]. In particular, we know from earlier works [3, 29] that for $\varepsilon = 0$, $p^\star_{optimal} = \frac{\mathbb{E}[S]}{\mathbb{E}[S]+\mathbb{E}[L]}$ and it is achieved by a Dirac delta distribution at $\mathbb{E}[S]$. We observed in the numerical results in Section IV that the presence of the parameter ε changes $p^\star$. For example, we have seen that if more load is absorbed from the overloaded lines by increasing ε, $p^\star$ may increase or decrease with respect to the case $\varepsilon = 0$. In cases when $p^\star$ increases $n_\infty(p,\varepsilon)$ decreases. It is, therefore, difficult to asses the robustness using only the $p^\star$ metric; e.g., see Fig. 7 where the distribution that leads to the highest $p^\star$ does not maximize the final system size $n_\infty(p,\varepsilon)$ uniformly across all attack sizes $0 \le p \le 1$.

In order to quantify the overall robustness of the network under all possible attack sizes, we consider a metric that measures the area under $n_\infty(p,\varepsilon)$ over $0 \le p \le 1$. Namely, we let

$$\mathcal{R}(\varepsilon) = \int_0^1 n_\infty(p,\varepsilon)\mathrm{d}p. \tag{12}$$

The metric $\mathcal{R}(\varepsilon)$ was introduced in [30], and can be seen [41] to represent the *expected* final system size in response to an attack whose size p is selected uniformly at random over $[0,1]$. It is in this spirit that the metric $\mathcal{R}(\varepsilon)$ quantifies the overall system robustness under a range of attack sizes for fixed ε. Alternative metrics can also be defined where the attack size p is drawn from an arbitrary distribution $F(p)$, e.g., to account for the fact that attacks of certain size might be more likely than others. In that case, we would again compute the mean of the final system size, i.e.,

$$\mathbb{E}_p\left[n_\infty(p,\varepsilon)\right] = \int_0^1 n_\infty(p,\varepsilon)\mathrm{d}F(p) \tag{13}$$

Clearly, $\mathcal{R}(\varepsilon)$ defined in (12) is recovered when $F(p)$ is the uniform distribution over $[0,1]$.

Our next result conclusively establishes that for any ε, the Dirac delta distribution [42] for free-space S optimizes the robustness of the system with respect to the metric $\mathcal{R}(\varepsilon)$ among all possible distributions $P_{LS}(x,y)$ with fixed $\mathbb{E}[S]$ and $\mathbb{E}[L]$. First, we note that if $p_{LS}(x,y) = p_L(x)\delta(y-\mathbb{E}[S])$, then the final system size is independent of ε. This is because after the initial attack, either all lines will fail (if $\mathbb{E}[S] \le p\mathbb{E}[L]/(1-p)$), or they will all survive and the cascades will not continue. Thus, the final system size under the Dirac-delta distribution of free-space is given [29] by

$$n_{\delta,\infty}(p) = \begin{cases} 1-p & \text{if } p < p_\delta^\star \\ 0 & \text{if } p \ge p_\delta^\star \end{cases} \tag{14}$$

where, the critical attack size $p_\delta^\star$ is given by

$$p_\delta^\star = \frac{\mathbb{E}[S]}{\mathbb{E}[S]+\mathbb{E}[L]}.$$

We will show that the distribution $p_{LS}(x,y) = p_L(x)\delta(y-\mathbb{E}[S])$ maximizes the robustness metric $\mathcal{R}(\varepsilon)$ among all p_{LS} with mean values for L and S are fixed at $\mathbb{E}[L]$ and $\mathbb{E}[S]$, respectively. In view of (14), this will follow if we show that

$$\int_0^1 n_\infty(p,\varepsilon,p_{LS})\mathrm{d}p \le \int_0^{p_\delta^\star}(1-p)\mathrm{d}p \tag{15}$$

where $n_\infty(p,\varepsilon,p_{LS}(x,y))$ denotes the final system size under attack size p, when load and free-space values of the lines are generated independently from the distribution $p_{LS}(x,y)$ (with fixed $\mathbb{E}[L]$, $\mathbb{E}[S]$).

From (8) we note that

$$\begin{aligned} n_\infty(p,\varepsilon,p_{LS}(x,y)) &\le (1-p)\mathbb{P}\left[S \ge Q_0\right] \\ &= (1-p)\mathbb{P}\left[S \ge \frac{p}{1-p}\mathbb{E}[L]\right], \end{aligned} \tag{16}$$

due to the fact that $Q_0 \le Q_t$ for all $t = 1,2,\ldots$. Therefore, we will get the desired result (15) if we show that

$$\int_0^1 (1-p)\mathbb{P}\left[S \ge \frac{p}{1-p}\mathbb{E}[L]\right]\mathrm{d}p \le \int_0^{p_\delta^\star}(1-p)\mathrm{d}p,$$

or, equivalently that

$$\begin{aligned} &\int_{p_\delta^\star}^1 (1-p)\mathbb{P}\left[S \ge \frac{p}{1-p}\mathbb{E}[L]\right]\mathrm{d}p \\ &\le \int_0^{p_\delta^\star}(1-p)\mathbb{P}\left[S < \frac{p}{1-p}\mathbb{E}[L]\right]\mathrm{d}p, \end{aligned} \tag{17}$$

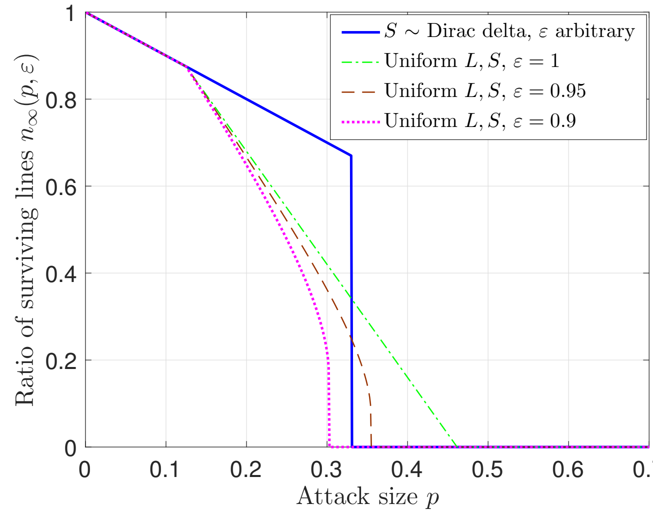

FIG. 7. *We plot the ratio of surviving lines $n_\infty(p,\varepsilon)$ as a function of the attack size p in the setting when L and S are independent and distributed uniformly as $U[0,120]$ and $U[10,60]$, respectively, as well as the setting when S is Dirac delta distributed as $\delta(x-\mathbb{E}[S])$.*

Since $1-p$ is monotone decreasing over the range $0 \le p \le 1$, and both $\mathbb{P}\left[S \ge \frac{p}{1-p}\mathbb{E}[L]\right]$ and $\mathbb{P}\left[S < \frac{p}{1-p}\mathbb{E}[L]\right]$ are non-negative, (17) will follow if we show that

$$\int_{p_\delta^\star}^1 \mathbb{P}\left[S \ge \frac{p}{1-p}\mathbb{E}[L]\right]\mathrm{d}p \le \int_0^{p_\delta^\star}\mathbb{P}\left[S < \frac{p}{1-p}\mathbb{E}[L]\right]\mathrm{d}p,$$

or, equivalently that

$$\int_0^1 \mathbb{P}\left[S \ge \frac{p}{1-p}\mathbb{E}[L]\right]\mathrm{d}p \le \int_0^{p_\delta^\star}\mathrm{d}p = \frac{\mathbb{E}[S]}{\mathbb{E}[S]+\mathbb{E}[L]}, \tag{18}$$

In order to establish (18), we make a change of variables $x = \frac{p}{1-p}\mathbb{E}[L]$ and write

$$\begin{aligned} &\int_0^1 \mathbb{P}\left[S \ge \frac{p}{1-p}\mathbb{E}[L]\right]\mathrm{d}p \\ &= \int_0^\infty \mathbb{P}\left[S \ge x\right]\mathrm{d}\left(\frac{x}{x+\mathbb{E}[L]}\right) \qquad (19) \\ &= \mathbb{P}\left[S \ge x\right]\frac{x}{x+\mathbb{E}[L]}\Big|_{x=0}^\infty - \int_0^\infty \frac{x}{x+\mathbb{E}[L]}\mathrm{d}(\mathbb{P}\left[S \ge x\right]) \\ &= \mathbb{E}\left[\frac{S}{S+\mathbb{E}[L]}\right] \\ &\le \frac{\mathbb{E}[S]}{\mathbb{E}[S]+\mathbb{E}[L]} \qquad (20) \end{aligned}$$

where we use integration by parts in (19) and apply Jensen's inequality in (20) for the function $\frac{x}{x+\mathbb{E}[L]}$ that is concave in x. This establishes (18) and the desired result (15) follows in view of the preceding arguments.

This result shows that the system's robustness with respect to the metric $\mathcal{R}(\varepsilon)$ (defined at (12)) is maximized under the constraints of fixed $\mathbb{E}[L]$ and fixed $\mathbb{E}[S]$ (and hence fixed $\mathbb{E}[C]$), by giving each line an equal free-space $\mathbb{E}[S]$, *irrespective of how the initial loads are distributed and the redistribution process in the later stages.* In other words, the robustness is maximized by choosing a line's capacity C_i through $C_i = L_i + \mathbb{E}[S]$ no matter what its load L_i is.

In Fig. 7, we plot the fraction of surviving lines $n_\infty(p,\varepsilon)$ as a function of the attack size p for several ε values, in the setting when L and S are independent and uniformly distributed as $U[0,120]$ and $U[10,60]$, respectively. We compare the corresponding final system size $n_\infty(p,\varepsilon)$ when S is Dirac delta distributed as $\delta(x-\mathbb{E}[S])$. We observe that the area under $n_\infty(p,\varepsilon)$ is larger under the Dirac delta distribution compared to other cases. In Fig. 8, we provide a comparison of the metric $\mathcal{R}(\varepsilon)$ for a family of Weibull distributions with fixed $\mathbb{E}[L]$ and $\mathbb{E}[S]$ while varying the scale parameter k of the distribution. We observe that $\mathcal{R}(\varepsilon)$ is monotone increasing in k and is maximized in the limiting case $k \to \infty$. This observation is in perfect agreement with our result given that the Weibull distribution approaches to a Dirac delta function as k goes to infinity.

In light of the results in Section IV, we conclude that the critical attack size $p^\star(\varepsilon)$ may be greater or less than $\frac{\mathbb{E}[S]}{\mathbb{E}[S]+\mathbb{E}[L]}$ depending on the specific distribution p_{LS} used (with fixed $\mathbb{E}[L]$ and $\mathbb{E}[S]$). In particular, we have seen that it is always possible to choose a marginal distribution with $\mathbb{E}[S]$ such that $p^\star$ is arbitrarily close to 1. Therefore, one might think that the area under $n_\infty(p,\varepsilon)$ while swiping all possible p could also increase when ε is increased and the system has the capability to absorb the extra load coming from the failing lines and eradicate the potentially detrimental effect of their failure to the overall system. Our result shows firmly that this intuition is incorrect and the metric $\mathcal{R}(\varepsilon)$ is maximized when the distribution of S is the Dirac delta function centered at $\mathbb{E}[S]$ irrespective of the distribution of L. We note that our argument follows from the facts that the extra load due to the initial attack $Q_0 = \frac{p}{1-p}\mathbb{E}[L]$ is monotone increasing, continuous, and convex in the initial attack size p. These properties are expected to hold in a large set of instances of this problem. Therefore, the optimality of the Dirac-delta distribution of S is likely to hold under more general cases where these properties hold.

We note that the optimality of the Dirac-delta distribution of S (in the sense of maximizing $\mathcal{R}(\varepsilon)$) holds irrespective of the value of ε. As such, this optimality prevails under any time variation in ε or possible dependence of ε on the instantaneous extra load per line Q_t. We also note that if the prior randomness $F(p)$ on the attack size p in (13) is assumed to have a monotone decreasing derivative, i.e., if higher attack sizes are *less likely*, then the Dirac-delta distribution of free-space S is still optimal with respect to the resulting metric in (13). Such cases occur in situations where the malicious attacker is more likely to choose smaller attack sizes due to resource or time constraints. We similarly observe that if the support of the prior distribution of p is contained in the interval $[0, \frac{\mathbb{E}[S]}{\mathbb{E}[S]+\mathbb{E}[L]}]$, then the Dirac-delta function at $\mathbb{E}[S]$ is optimal with respect to $\mathcal{R}(\varepsilon)$.

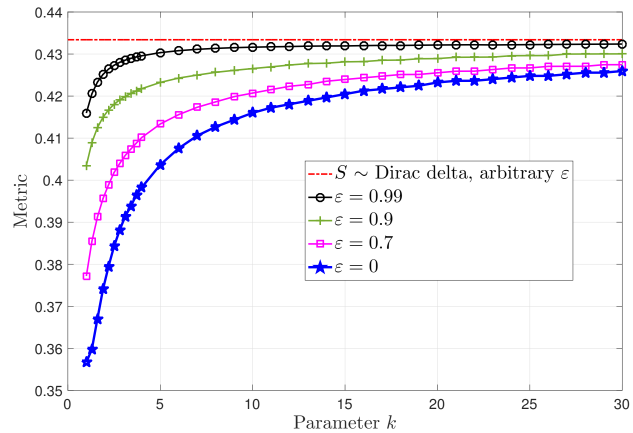

FIG. 8. *$L_1, \ldots, L_N$ are drawn from Weibull distribution with $L_{min} = 1$ and k, λ such that $\mathbb{E}[L] = 2$ and $S = 1.74L$. We plot the metric $\mathcal{R}(\varepsilon)$ in (12) as a function of the parameter k.*

While it is hard to generalize the optimality of Dirac delta function for $0 < \varepsilon < 1$ and any prior distribution on p, we observe that if p is deterministic and $\varepsilon = 1$, then the robustness metric in (13) is given by

$$\mathbb{E}_p[n_\infty(p,\varepsilon)] = n_\infty(p,1) = (1-p)\mathbb{P}[S > Q_0]. \quad (21)$$

Then, in order to maximize $n_\infty(p,\varepsilon)$, it suffices to minimize $\mathbb{P}[S > Q_0] = \mathbb{P}[S > p\mathbb{E}[L]/(1-p)]$ subject to $\mathbb{E}[S]$ being fixed. If the known attack size satisfies $p \le \frac{\mathbb{E}[S]}{\mathbb{E}[S]+\mathbb{E}[L]}$, then this is achieved when the distribution of S is given by the Dirac-delta function centered at $\mathbb{E}[S]$. If, on the other hand, we have $p > \frac{\mathbb{E}[S]}{\mathbb{E}[S]+\mathbb{E}[L]}$, then the optimal distribution of S consists of two Dirac delta functions centered at 0 and $\frac{p}{1-p}\mathbb{E}[L]$, respectively, with appropriate probabilities selected such that the mean value is $\mathbb{E}[S]$. In other words, if the attack size is larger than what can be resisted by giving each line an equal amount $\mathbb{E}[S]$ of free-space, then it is optimal to give a fraction of lines *zero* free-space, while giving each of the other lines an equal amount of $\frac{p}{1-p}\mathbb{E}[L]$ free-space; i.e., just enough so that they can handle the additional load of Q_0 that will be shed on them after the attack.

VI. CONCLUSION

We studied the robustness of flow networks consisting of N lines against random attacks under a partial load redistribution model. In particular, when a line fails due to overloading, it is removed from the system and (1ε)-fraction of the load it was carrying gets redistributed equally among all remaining lines while the remaining ε-fraction is assumed to be lost or absorbed. We derive recursive relations describing the dynamics of cascading failures for any attack size p, and identify the *final* fraction of surviving lines when the cascades stop. These findings are confirmed via extensive simulations. Among other things, we show that unlike the full redistribution case (i.e., $\varepsilon = 0$), partial redistribution might lead to the order of transition at the critical attack size $p^\star$ changing from first to second-order.

One of the most interesting findings of this paper is concerned with how system robustness can be *maximized* by properly choosing the distribution p_{LS} that generates the initial load and free-space values of each line. We consider this problem when the mean load $\mathbb{E}[L]$ and mean free-space $\mathbb{E}[S]$ are fixed. First, we show that unlike the full redistribution case (i.e., when $\varepsilon = 0$), the critical attack size $p^\star$ is not necessarily maximized by assigning every line the same free-space $\mathbb{E}[S]$; depending on the fraction ε of the load that is absorbed at each stage, we see that distributions other than Dirac-delta for S may lead to higher critical points $p^\star$. Next, we consider the robustness metric proposed in [30] that computes the *area* under the final system size $n_\infty(p, \varepsilon)$ over all possible attack sizes $0 \leq p \leq 1$; this amounts to computing the average response of the network to initial attacks of different size. We show that the system is most robust in the sense that the area metric is maximized, when the variation among the free-space of lines is minimized. In other words, the Dirac- delta distribution of free-space leads to the optimum robustness, irrespective of ε and how load L is distributed.

There are many open problems one can consider for future work. For instance, the analysis can be extended to the case where the redistribution parameter ε is not the same for all lines, but follows a given probability distribution. Similarly, ε could be a time-varying parameter or it could depend on the extra load per line in the current stage. Such possibilities would allow us to obtain further understanding on the dynamical properties of the cascading failures and the mechanisms that could lead to a smooth failure. Additionally, it would be interesting to see if the robustness is still maximized with a Dirac delta type distribution on the free-space under various combinations of possibilities on ε. Finally, it would be interesting to study the partial redistribution model under *targeted* attacks rather than random failures.

ACKNOWLEDGMENTS

This research was supported in part by National Science Foundation through grant CCF #1422165, and in part by the Department of Electrical and Computer Engineering at Carnegie Mellon University.

[1] S. Tang, J. Yuan, X. Mao, X.-Y. Li, W. Chen, and G. Dai, in *Proceedings of IEEE INFOCOM 2011* (2011) pp. 2291 –2299.

[2] H. Wu, A. Arenas, and S. Gómez, Physical Review E **95**, 012301 (2017).

[3] O. Yağan and V. Gligor, Physical Review E **86**, 036103 (2012).

[4] Y. Zhuang and O. Yağan, IEEE Transactions on Network Science and Engineering **3**, 211 (2016).

[5] O. Yağan, D. Qian, J. Zhang, and D. Cochran, IEEE Journal on Selected Areas in Communications **31**, 1038 (2013).

[6] R. Parshani, S. V. Buldyrev, and S. Havlin, Phys. Rev. Lett. **105** (2010).

[7] S.-W. Son, G. Bizhani, C. Christensen, P. Grassberger, and M. Paczuski, EPL (Europhysics Letters) **97**, 16006 (2012).

[8] B. Min, S. Do Yi, K.-M. Lee, and K.-I. Goh, Physical Review E **89**, 042811 (2014).

[9] K.-M. Lee, C. D. Brummitt, and K.-I. Goh, Physical Review E **90**, 062816 (2014).

[10] C. Wu, S. Ji, R. Zhang, L. Chen, J. Chen, X. Li, and Y. Hu, EPL (Europhysics Letters) **107**, 48001 (2014).

[11] F. Radicchi, Nature Physics **11**, 597 (2015).

[12] O. Yağan, D. Qian, J. Zhang, and D. Cochran, IEEE Transactions on Parallel and Distributed Systems **23**, 1708 (2012).

[13] X. Huang, J. Gao, S. Buldyrev, S. Havlin, and H. E. Stanley, Phys. Rev. E **83** (2011).

[14] S. V. Buldyrev, R. Parshani, G. Paul, H. E. Stanley, and S. Havlin, Nature **464**, 1025 (2010).

[15] W. Li, A. Bashan, S. V. Buldyrev, H. E. Stanley, and S. Havlin, Physical review letters **108**, 228702 (2012).

[16] S. V. Buldyrev, R. Parshani, G. Paul, H. E. Stanley, and S. Havlin, Nature **464**, 1025 (2010).

[17] J. Gao, S. V. Buldyrev, S. Havlin, and H. E. Stanley, Physical Review Letters **107**, 195701 (2011).

[18] C. D. Brummitt, R. M. DSouza, and E. Leicht, Proceedings of the National Academy of Sciences **109**, E680 (2012).

[19] I. Dobson, B. A. Carreras, V. E. Lynch, and D. E. Newman, Chaos: An Interdisciplinary Journal of Nonlinear Science **17**, 026103 (2007).

[20] M. Elliott, B. Golub, and M. O. Jackson, American Economic Review **104**, 3115 (2014).

[21] G. Zhang, Z. Li, B. Zhang, and W. A. Halang, Physica A: Statistical Mechanics and its Applications **392**, 3273 (2013).

[22] S. Pahwa, C. Scoglio, and A. Scala, Scientific reports **4** (2014).

[23] H. Daniels, Proceedings of the Royal Society of London. Series A. Mathematical and Physical Sciences **183**, 405 (1945).

[24] J. V. Andersen, D. Sornette, and K.-t. Leung, Phys. Rev. Lett. **78**, 2140 (1997).

[25] O. Yağan, Phys. Rev. E **91**, 062811 (2015).

[26] W. Curtin, Journal of the Mechanics and Physics of Solids **41**, 217 (1993).

[27] F. Kun, M. Costa, R. Costa Filho, J. Andrade Jr, J. Soares, S. Zapperi, and H. Herrmann, Journal of Statistical Mechanics: Theory and Experiment **2007**, P02003 (2007).
[28] D. Cohen, P. Lehmann, and D. Or, Water resources research **45** (2009).
[29] Y. Zhang and O. Yağan, Scientific reports **6** (2016).
[30] C. Schneider, A. J. J. H. S. Moreira, A.A., and H. Herrmann, Proceedings of the National Academy of Sciences **108**, 3838 (2011).
[31] A. E. Motter and Y.-C. Lai, Phys. Rev. E **66**, 065102 (2002).
[32] W.-X. Wang and G. Chen, Phys. Rev. E **77**, 026101 (2008).
[33] B. Mirzasoleiman, M. Babaei, M. Jalili, and M. Safari, Physical Review E **84**, 046114 (2011).
[34] P. Crucitti, V. Latora, and M. Marchiori, Phys. Rev. E **69**, 045104 (2004).
[35] (2004).
[36] P. Palensky and D. Dietrich, IEEE transactions on industrial informatics **7**, 381 (2011).
[37] D. Sornette, K.-T. Leung, and J. Andersen, arXiv preprint cond-mat/9712313 (1997).
[38] S. Pradhan and B. K. Chakrabarti, International Journal of Modern Physics B **17**, 5565 (2003).
[39] C. Roy, S. Kundu, and S. Manna, Physical Review E **91**, 032103 (2015).
[40] R. Parshani, S. V. Buldyrev, and S. Havlin, Physical review letters **105**, 048701 (2010).
[41] The metric in [30, Equation 1] is introduced as the sum of surviving nodes over all possible number of attacked lines. One can show by the almost sure convergence of the probabilities to the fraction of line failures due to the law of large numbers and the bounded convergence theorem that the metric $\mathcal{R}(\varepsilon)$ in (12) represents the same metric in [30] as the number of lines N grows.
[42] We note that Dirac delta distribution can be viewed as a limiting distribution for family of continuous distributions and therefore it can be treated within the framework of our paper that assumed continuous $P_{LS}(x, y)$.